ELSEVIER

Contents lists available at ScienceDirect

Materials Chemistry and Physics

journal homepage: www.elsevier.com/locate/matchemphys



Design of transparent and superhydrophobic PDMS–silica coatings for sustainable photovoltaic applications

Sagar S. Ingole^a, Sudarshan N. Khutale^a, Akshay R. Jundle^a, Pradip P. Gaikwad^a, Rutuja A. Ekunde^a, Rajaram S. Sutar^b, Shanhu Liu^{b,*}, Sanjay S. Latthe^{a,**}

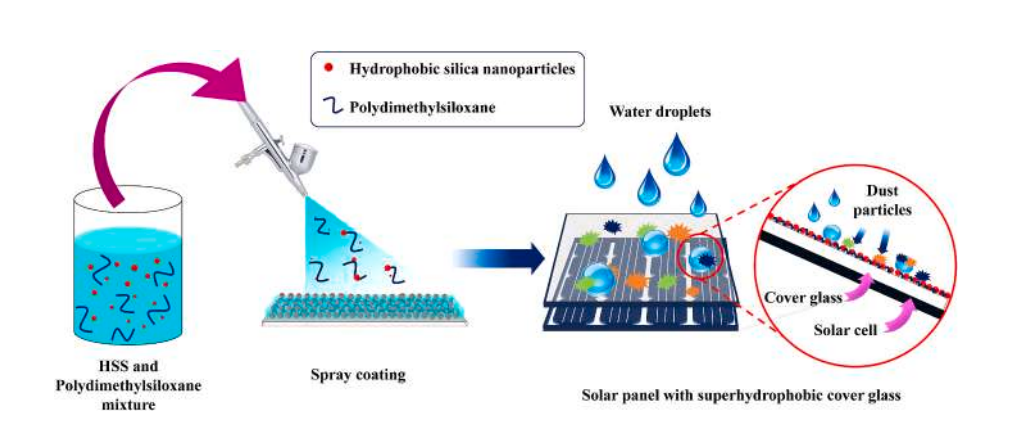
HIGHLIGHTS

- A highly transparent superhydrophobic coating was developed via a single-step spray process.
- PDMS and hydrophobic silica nanoparticles were synergistically used to achieve dual functionality.
- Coated samples showed excellent water repellency (WCA $\sim 165^{\circ}$) with > 85% optical transparency.
- Surface roughness and wetting attributions were tuned by adjusting PDMS concentration.
- Self-cleaning coating reduced dust accumulation and maintained solar cell efficiency in real-time photovoltaic test.

ARTICLE INFO

Keywords: Superhydrophobic Self-cleaning Solar cell cover glass Transparency Contact angle

$G\ R\ A\ P\ H\ I\ C\ A\ L\ A\ B\ S\ T\ R\ A\ C\ T$



ABSTRACT

Solar panels encounter challenges from environmental factors, such as dirt, dust, and debris that block sunlight, requiring regular cleaning, especially in arid areas. Issues like bird droppings, extreme weather, and coastal salt air can also corrode panels and reduce energy output. In this study, we focused on creating an innovative coating by employing a suspension of hydrophobic silica sol (HSS) in combination with polydimethylsiloxane (PDMS) on glass substrate using a facile spray deposition technique. To optimize the transparency and superhydrophobicity of the coatings, the concentration of PDMS was varied while maintaining a constant amount of HSS in the suspension. The optimal formulation achieved transparency of 87.52 % within the wavelength range of 350-1100 nm, which is essential for applications in solar energy technology. In addition, the coating demonstrating exceptional water repellency with water contact angle (WCA) of $165.14 \pm 1.41^\circ$, coupled with a minimal sliding angle (SA) of less than $1.33 \pm 0.29^\circ$. Moreover, the coatings sustain their durability over standardized tests, including adhesive tape, sandpaper abrasion, and exposure to different pH solutions, confirming their suitability for practical applications. Additionally, their self-cleaning capabilities proved effective under harsh conditions, effectively repelling dirt and contaminants. This coating has significant potential for protecting solar

E-mail addresses: liushanhu@vip.henu.edu.cn (S. Liu), latthes@gmail.com (S.S. Latthe).

^a Self-cleaning Research Laboratory, Department of Physics, Vivekanand College (An Empowered Autonomous Institute), (Affiliated to Shivaji University, Kolhapur), Kolhapur, 416003. Maharashtra. India

^b College of Chemistry and Molecular Science, Henan University, Kaifeng, 475004, People's Republic of China

^{*} Corresponding author.

^{**} Corresponding author.

cells against environmental contaminants such as dust, moisture and pollutants, thereby improving their longevity and efficiency in energy harvesting, which could enhance the overall effectiveness of solar technologies.

1. Introduction

Solar panels face various challenges due to continuous exposure to outdoor environmental factors and wear. Accumulation of dirt, dust, and debris can block sunlight, making regular cleaning essential, particularly in arid regions. Additionally, bird droppings and stains can create spots that reduce energy output and require maintenance. Extreme weather conditions such as hail, snow, high winds, and heavy rain can affect panel performance by causing surface contamination over time. In coastal areas, salt air can corrode metal components, while moisture in the junction box may lead to electrical shorts. Regular inspections and cleaning are necessary to help mitigate these issues, although this process can be labour-intensive and financially demanding. To address these challenges, transparent superhydrophobic coatings have emerged as a promising solution for solar panels. These coatings, inspired by natural surfaces like lotus leaves, combine water repellency with optical clarity [1]. They have gained considerable attention due to their exceptional water-repellent and self-cleaning properties. These unique coatings minimize water adhesion and reduce contamination, making them particularly effective for use in optics, electronics, and energy devices [2]. One of the key benefits of these superhydrophobic coatings is that they cause water droplets to form nearly perfect spheres on their surface, resulting in a high-water contact angle (greater than 150°) as well as a low sliding angle (less than 10°). As a result, water droplets do not stick to the surface: instead, they carries dust and other contaminants readily during roll off the surface which eventually keeps the surface clean [3]. Consequently, superhydrophobic coatings have found various applications, which includes different abilities such as anti-fogging [4], anti-icing [5], oil-water separation [6], and in photothermal actuators [7]. A transparent superhydrophobic coating is challenging to fabricate because it requires a synergic balance between transparency and water-repellent properties, as these often compete with each other [8]. An elevation in surface roughness enhances the hydrophobicity of the coating on the other hand lowers the light transmittance due to increased light scattering. This happens due to Mie scattering [9] of the light due to high agglomeration of the particles in localized regions [10]. The transparent self-cleaning coating have been achieved via various methods such as aerosol assisted chemical vapor deposition [11], sol-gel [12], spray coating [13] spin coating [14], dip coating [15], micro-stereolithography [16].

In recent years, several research groups have developed not only transparent but also self-cleaning superhydrophobic coatings on glass surfaces. For instance, Liu et al. have fabricated transparent selfcleaning coating using hydrophobic silica nanoparticles (ranging from 7 to 40 nm) through dip coating [15]. This coating achieved a WCA of 164° and a very low sliding angle (SA) of 1°, along with a transparency of 91.4 %. Similarly, Liang et al. have developed a transparent coating using silica nanoparticles (an average diameter of 15 ± 5 nm) combined with PDMS via spin coating, achieving a WCA of 158° and a transmittance greater than 80 % in the visible range [14]. The resulting sample demonstrated good performance in mechanical tests, including thermal stability (ranging from −15 to 450 °C) and resistance to water flow impact (20 L). It also exhibited excellent chemical stability when exposed to acidic, alkaline, or saline environments. Syafiq et al. have developed transparent, hydrophobic self-cleaning coating on glass by modifying PDMS with 3-aminopropyltriethoxysilane (APTES) via a dip coating process [17]. A stable hybrid coating was formed due to the cross-linking of the flexible amino groups in APTES, which facilitated silica structuration within the PDMS chains. This coating achieved a WCA of 103.9° while maintaining over 90 % optical transparency in the visible range. Ariadne et al. have fabricated transparent and superhydrophobic coatings by spraying room temperature vulcanized (RTV) polysiloxane matrices loaded with organically modified silica (ORMO-SIL) nanoparticles [18]. The various coatings were fabricated with R202 (hydrophobic silica functionalized with PDMS), R200.NFS (silica functionalized with (1H,1H,2H,2H nonafluorohexyl)-triethoxysilane) and R200.OTSNFS (hybrid functionalization with octyl-triethoxy-silane and (1H,1H,2H,2H nonafluorohexyl)-triethoxysilane). Among these, the coating contained with 25 % of R200.OTSNFS demonstrated higher WCA of 165° and low SA of 1.2° along with 54 % of transparency.

Besides, the HDMS possess as an effective hydrophobic modifier for silica. Li et al. have developed a bilayer coating utilizing HMDSmodified silica in conjunction with epoxy-modified silicone/fumed silica to enhance the optical transparency and water-repellency of glass surfaces through a dip-coating process [19]. This bilayer demonstrated a transparency improvement of 4.3 % compared to untreated glass, achieving a remarkable WCA of 155.1° and a SA of just 0.1°, indicative of superior self-cleaning properties. The cross-linking properties of the silicone resin conferred long-term stability under aggressive environmental conditions. In another study, Salehi et al. have used a spray technique to apply a dispersion of HMDS-modified silica nanoparticles combined with PDMS, resulting in a transparent, superhydrophobic thin coating on glass substrates [20]. This coating exhibited an impressive average transmittance of about 96 % and a WCA near 96° with SA of 5°. Saeedi et al. have fabricated transparent hydrophobic and anti-icing coatings by integrating PDMS with SiO2 nanoparticles that had been modified with MTMS and HMDS [21]. In comparison of MTMS modified SiO₂ and PDMS coating, the resultant HDMS modified SiO₂ and PDMS coatings achieved a transparency of 93.7 % and a WCA of 107 \pm 1° and SA of $\sim 25^{\circ}$. Notably, these coatings extended the icing duration for water droplets from 270 s to 710 s, attributed to the reduced surface energy imparted by the modified SiO₂ nanoparticles. The HDMS-modified SiO₂ and PDMS composite coatings demonstrate excellent transparency and superhydrophobic self-cleaning properties. However, achieving a synergistic effect among these components is challenging, especially under harsh conditions like abrasion, alkaline-acidic exposure, and contaminants. Further research is needed to better understand these interactions and improve the coatings' stability, while preserving their beneficial characteristics.

In the present study, we have synthesized SiO_2 nanoparticles through the sol-gel process and subsequently modified them with HDMS. The coating composite was prepared by dispersing HDMS-modified SiO_2 nanoparticles in a PDMS solution, followed by a single-step spray method to develop a self-cleaning coating on glass substrates. This coating was further tested for practical applications on solar cells. The modified SiO_2 nanoparticles ensure not only hydrophobicity but also uniform dispersion within the PDMS solution. This customization enabled the creation of a well-structured hierarchical surface, resulting in superior water-repellent properties for the coatings. Further, a comprehensive study was conducted to evaluate the coatings' characterizations and their mechanical and chemical properties, as well as their self-cleaning and photovoltaic performances.

2. Experimental

2.1. Materials

Tetraethylorthosilicate (TEOS, 98 %) was purchased from Sigma Aldrich (Bangalore, India). Ammonia (NH₄OH, \sim 25 % NH₃) was purchased from Thomas baker private limited (Ambernath, India).

Polydimethylsiloxane (PDMS, viscosity 5 cSt) and Hexamethyldisilazane (HMDS) were acquired from Sigma-Aldrich (USA). Ethanol (anhydrous, 99.9 %) and hexane were purchased from Spectrochem private limited (Mumbai, India). The glass substrates ($75 \times 25 \times 1.35 \text{ mm}^3$) were purchased from Riviera Glass private limited (Mumbai, India).

2.2. Preparation of hydrophobic silica sol (HSS)

A synthesis of hydrophobic silica sol was synthesized by adding 0.6 mL of TEOS and 0.6 mL of NH₄OH dropwise into 10 mL of ethanol. This solution was stirred at 500 rpm for 1 h while maintaining a temperature of 60 °C. After 10 min of stirring, the colour of solution was changed from transparent to sky blue. After 1 h of stirring, 0.4 mL of HMDS was added dropwise, and the solution was stirred for an additional 2 h. After this stirring period, the mixing was halted, but the heating continued for the next 2 days to ensure the complete modification of the silica nanoparticles from hydrophilic to hydrophobic. This solution is referred to as hydrophobic silica sol (HSS). The entire process was carried out in the round bottomed flask and completely closed by its cap to minimize the solvent loss as well as moisture ingress. To determine the particle sizes of the bare silica nanoparticles and HMDS-modified silica nanoparticles, a FE-SEM analysis with histograms were performed for dip coated samples of both solutions.

2.3. Fabrication of superhydrophobic coating

To remove dirt and contaminants, the glass substrates were initially washed with Labolene (a laboratory detergent). After washing, the glass slides were subjected to ultrasonication in ethanol and distilled water for 10 min each, sequentially. Following ultrasonication, the glass

substrates were placed in oven at 100 °C for 10 min, after that they were used for the coating process. A 1 % v/v PDMS-hexane stock solution was prepared by dissolving $60 \mu L$ of PDMS in 6 mL of hexane and preserved in a glass bottle. To fabricate a superhydrophobic coating on the glass substrates, the prepared HSS was mixed with the polymeric solution through stirring for 1 h. The final solution was then sprayed (approximately 1 mL) onto the glass substrates (measuring 7 cm \times 2.5 cm) from a distance of 10 cm, using a nozzle with a diameter of 0.3 mm. The coated substrates were dried in oven at 150 °C for 2 h. The coatings were fabricated with 0, 100, 200, and 300 μL of the stock PDMS solution and a constant 1.5 mL of HSS to optimize the binder concentration. The resulting samples were designated as SP-0, SP-1, SP-2, and SP-3, respectively. Using the constant silica mass from the 1.5 mL HSS (\sim 0.0242 g) and converting PDMS volume to mass with PDMS \approx 0.965 g/mL, the PDMS:Silica mass ratios in the sprayed dispersions were 0, 0.0399:1, 0.0797:1, and 0.1195:1 for SP-0, SP-1, SP-2, and SP-3 sample, respectively. Fig. 1 depicts the schematic of the fabrication process.

2.4. Characterizations

A Field Emission Scanning Electron Microscope (FE-SEM, JEOL, JSM-7610F, Tokyo, Japan) was utilized to examine the surface morphology of the prepared coatings. The chemical composition of the samples was analyzed using Fourier-transform infrared spectroscopy (FT-IR, Magna-IR 560, Nicolet) and X-ray Photoelectron Spectroscopy (XPS, Escalab 250Xi, USA). Surface roughness was determined with a stylus profiler (Mitutoyo, SJ 210, Sakado, Japan), while optical transparency was measured using a UV-VIS spectrophotometer (UV-1900i, Shimadzu, India). The water contact angle (WCA) and sliding angle (SA) were assessed at three different locations on each sample using a contact

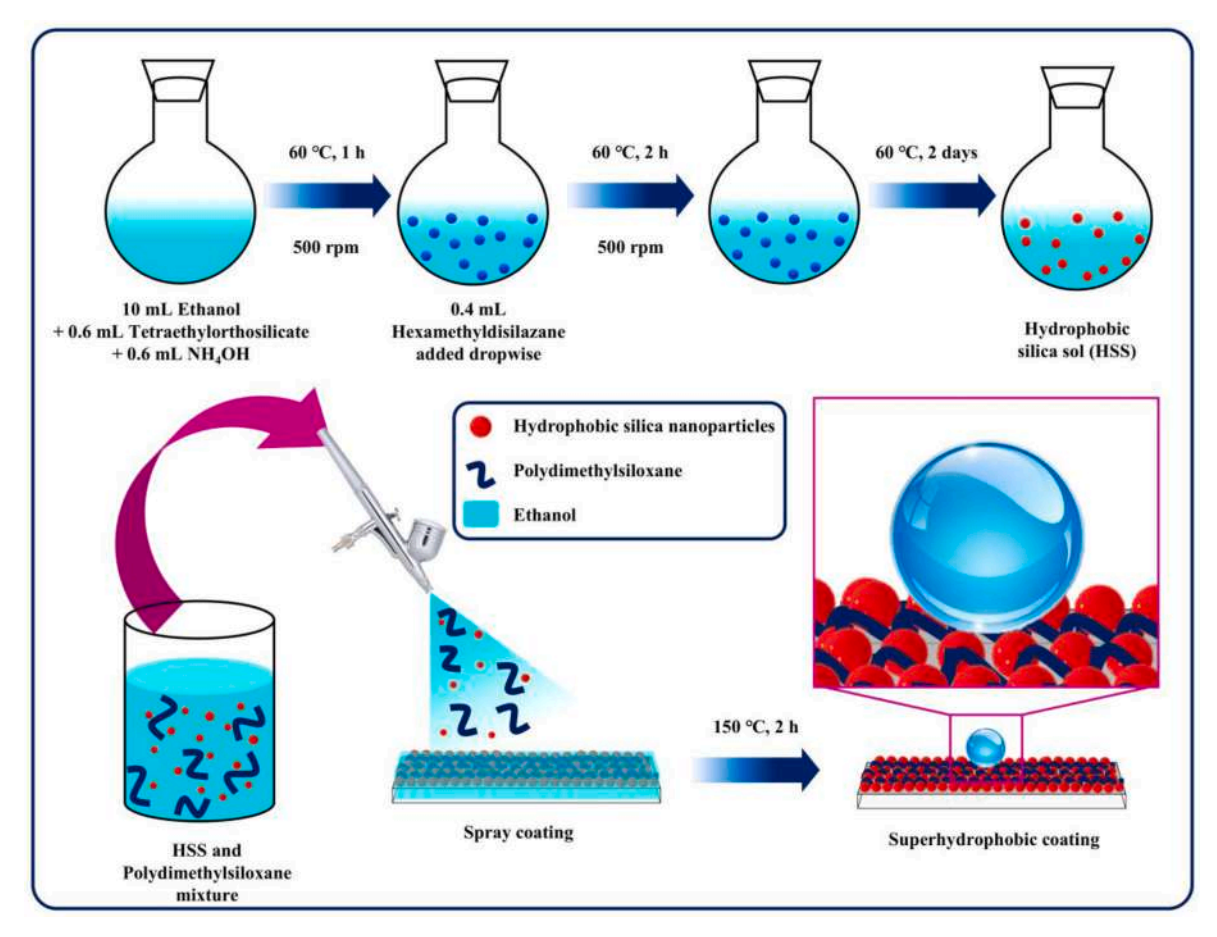


Fig. 1. Schematic of fabrication of superhydrophobic coatings on glass substrate by spray technique.

angle meter (HO-IAD-CAM-01, Holmarc Opto-Mechatronics Pvt. Ltd., Kochi, India). The final values reported were accompanied by the standard deviation (SD) for each sample.

2.5. Durability tests

An adhesive tape peeling and sandpaper abrasion tests were conducted on HSS and SP-2 coatings to assess the contribution of the PDMS binder to the coatings. Other durability tests, including the water droplet impact, sand particle impact, pencil hardness tests, and the effects of acidic and alkaline solutions, were performed on the SP-2 sample. For the adhesive tape test, Premier³⁸ tape (purchased from Amazon, India) was applied to the samples. A 50 g circular metal block was rolled over the tape to enhance the adhesion between tape and coating. The action of tape peeling was carried out at a constant speed of 0.36 cm/s. During sandpaper abrasion, a 1500 grit sandpaper was utilized to evaluate the robustness of the coatings. The coated surfaces of the samples were placed on the rough side of the sandpaper, with a 20 g weight positioned on top. The sample was dragged at an average speed of approximately 1 cm/s for a distance of 15 cm. For the water droplet impact test, a droplet of approximately 43 µL was dropped onto the sample from a height of 25 cm at a speed of 100 cm/s, while SP-2 sample being tilted at a 45° angle. Also, SP-2 sample was also positioned at a 45° angle from horizontal surface and sand particles (of diameter 25-50 µm) were released from the same height, falling at a speed of 25 cm/s. An adjustable Pencil Hardness Tester (Biuged, India) was used to evaluate the robustness of the coatings. Acid and alkaline solutions of pH values 2 and 12 were prepared by adding hydrochloric acid (HCl) and ammonia to distilled water respectively. Then samples were immersed in both pH solutions for 30 min. After immersion period, samples were dried at 60 °C for 20 min before characterization. The self-cleaning properties of the coatings were examined by using charcoal powder and red-dyed water. Additionally, a photovoltaic study was performed on a solar cell (99 mm \times 69 mm, purchased from Amazon, India) with spray coated glass using the SP-2 solution and used as cover glass to solar cell.

3. Results and discussion

3.1. Reaction mechanism

A highly stable silica dispersion was prepared using a modified Stöber process. Initially, the hydroxide (OH⁻) ions from ammonium hydroxide attack the tetraethyl orthosilicate (TEOS) molecule, replacing one of its ethoxy groups. This hydrolysis process is accelerated in a basic medium, facilitating the formation of silicate ions such as (SiO(OH)₃) and $(SiO_2(OH)_2)^{2-}$ [22]. Additionally, ammonium hydroxide promotes the deprotonation of silanol groups (Si-OH), creating more reactive Si-O- species that can undergo condensation reactions. At the 60 °C temperature, the rates of not only hydrolysis but also condensation were enhanced. This increased reactivity of the silica precursors leads to a greater number of nucleation sites and promotes the growth of silica nanoparticles. In a strongly basic environment, the silica nanoparticles acquire negative charges on their surfaces, resulting in higher stability due to increased electrostatic repulsion between individual nanoparticles, thereby preventing agglomeration. Furthermore, the surface of the silica nanoparticles is modified by trimethylsilyl ((CH₃)₃Si) groups from the HMDS molecule through a silanization process. During this process, ammonia is released as a byproduct, which further enriches the basic environment and stabilizes the functional properties of the silica nanoparticles. After the addition of PDMS (polydimethylsiloxane) to the trimethylsilyl-terminated silica suspension, the PDMS molecules physically adsorb the functionalized silica nanoparticles through hydrophobic and van der Waals interactions, resulting in a composite solution. The methyl groups from both the PDMS and the functionalized silica nanoparticles are responsible for forming a stable, uniform dispersion. During spray deposition, the atomized suspension is deposited onto a

glass substrate. At the stage of solvent evaporation, the polymeric content infiltrates the interparticle gaps which immobilize the silica particles in a PDMS matrix, creating a hierarchical rough structure [23].

3.2. Surface morphology and wettability

Figs. 2 and 3 illustrates the surface morphology and wettability (WCA and SA) of various samples. The FE-SEM images reveal that the agglomeration of HMDS-modified silica nanoparticles (less than 100 nm) led to the formation of micro-nano protrusions (bumps) and voids within the PDMS matrix. As depicted in Fig. S1, the FE-SEM image of dip-coated bare silica nanoparticles (S1a) extended to larger size after surface modification by HMDS (S1b). An average particle size of bare silica was 39 nm which extended to 61 nm for HMDS-modified silica nanoparticles. The corresponding particle histograms shows the particle distribution with dominant increase in size obtained from 35 to 40 nm (bare silica) to 50-60 nm (HMDS-modified silica) under the identical conditions. In case of SP-0 sample reveals the very less structural integrity. The silica nanoparticles seem to loosely distributed which formed weak clusters resulting in a fragile coating formation. On the other hand, with addition of the 100 µL PDMS in SP-1, the silica nanoparticles were started to held together and formed compact structure which also improves the adhesion with substrate. The SP-2 sample (200 μL PDMS) shows a uniform as well as well-distributed morphology than any other sample. The silica nanoparticles were strongly embedded in PDMS and able to produce ideal micro-nano rough structure. This balance between silica nanoparticles and PDMS makes SP-2 as optimized sample. However, further increase in PDMS loading to 300 µL (SP-3 sample), the gap between nanoparticles were filled out due to excess polymeric content and smoothens the surface. The WCA of bare glass, measured at $17.289 \pm 0.643^{\circ}$, was increased to over 150° after spraying the HSS-PDMS composite suspension. The fabricated samples, SP-0, SP-1, SP-2, and SP-3, exhibited WCA values of 160.43 \pm 0.06°, 162.17 \pm $1.12^{\circ},\,165.14\pm1.41^{\circ},\,$ and $136.9\pm2.7^{\circ},\,$ respectively. The SA values for these samples were recorded as 1.33 \pm 0.29°, 0.83 \pm 0.29°, and 1.33 \pm 0.29°, while the SP-3 sample showed no measurable SA, even when tilted downward. Additionally, an inset image in Fig. 3a displays various color-dyed water droplets placed on the SP-2 sample, which maintain a nearly spherical shape. A solid fraction (f) also calculated by using below formula.

 $\cos \theta app = f \cos \theta + (1 - f)\cos \theta air$

Where, $\theta_{app}\!:$ Apparent water contact angle, 0: Intrinsic WCA of the material, $\theta_{air}\!:$ WCA on air $=180^\circ$

Since $\cos\theta_{air} = -1$, the equation becomes:

 $\cos \theta app = f \cos \theta - (1 - f)$

Rearranging for f:

$$f = \frac{\cos \theta app + 1}{\cos \theta + 1}$$

The calculated solid fractions are mentioned for all samples in below Table 1.

Further, the solid content in the sprayed dispersion were calculated based on a fixed mass of silica produced within 1.5 mL of HSS and utilized PDMS stock solution [24]. These values are summarized in Table 1.

The roughness data are consistent with the measured WCA and are illustrated in Supplementary Fig. S2. The incorporation of PDMS into the hydrophobic silica sol enhanced the stability of the suspension. This improvement resulted from the steric hindrance provided by the PDMS chains, which prevented particle aggregation. Additionally, PDMS acted as a surface modifier, further increasing the hydrophobicity of the silica nanoparticles and resulting in their uniform dispersion within the sol. Consequently, a uniform hierarchical structure was achieved in the SP-2 sample, as depicted in Fig. 2(e and f) [25,26].

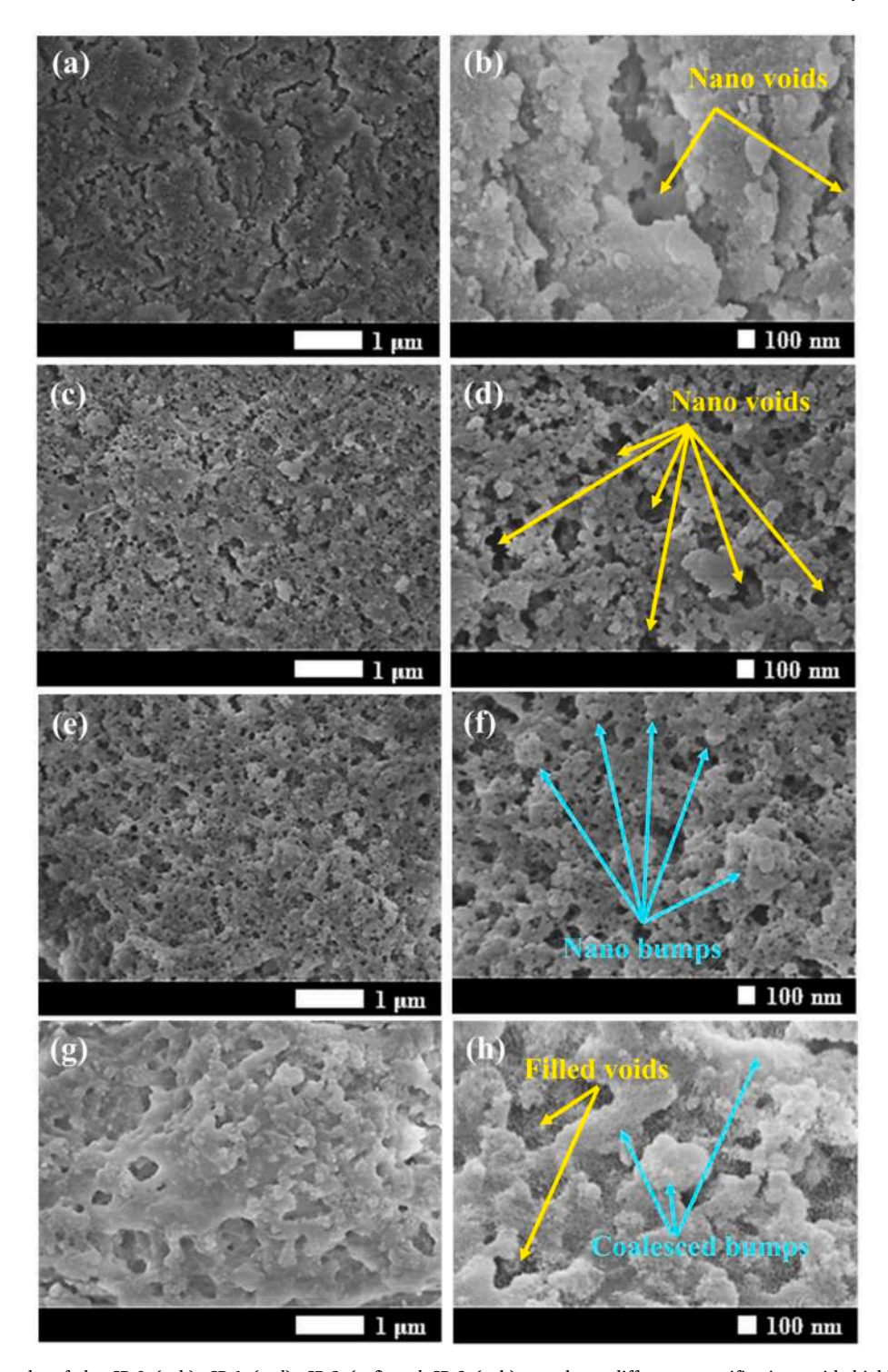


Fig. 2. FE-SEM micrographs of the SP-0 (a-b), SP-1 (c-d), SP-2 (e-f) and SP-3 (g-h) sample at different magnifications with highlighting nano-voids and nano-bumps.

The optimized SP-2 sample indicated the formation of a Cassie-Baxter state. An increase in PDMS content in the hydrophobic silica sol led to more adsorption onto the hydrophobic silica nanoparticles, which, in turn, increased the viscosity of the sol. This elevated viscosity slowed down the Brownian motion of individual particles, leading to the formation of clusters within the sol. As a result, a filling of micro and nano gaps and coalescence of bumps with the PDMS matrix (as shown in Fig. 2g and h), which contributed to a decrease in the WCA of the coatings. This reduction in WCA confirms the transition from the Cassie-Baxter state to the Wenzel state due to an increase in the solid-liquid

contact area, causing the water droplet to stick firmly to the surface. On the other hand, SP-0 sample which did not contain PDMS, exhibited significant agglomeration of silica nanoparticles (Fig. 2a and b) due to shrinkage of the coating during heat treatment. This shrinkage occurred through capillary forces while the solvent evaporated and the solid content reached a supersaturated state. The previous findings align with this surface morphology [27–30]. Furthermore, a non-wetting performance test was conducted on the SP-2 sample using a contact angle meter. As illustrated in Fig. 3b1-b3, a 10 μL droplet was allowed to make contact with the sample by lowering it down. After contact, the water

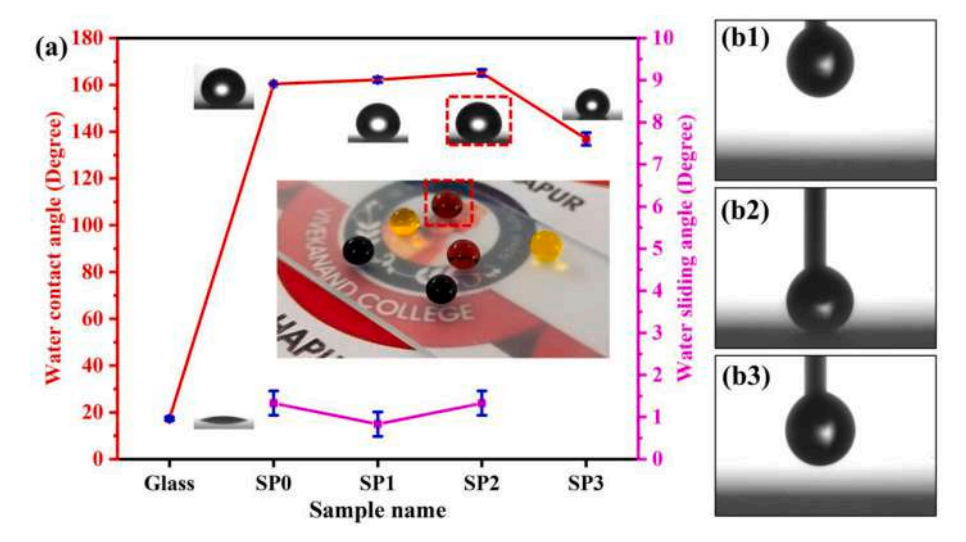


Fig. 3. (a) WCA and SA of different samples and an inset optical image of various color dyed water droplets placed on the SP-2 sample. (b1-b3) Non-wetting performance of the water droplet on SP-2 sample. (For interpretation of the references to color in this figure legend, the reader is referred to the Web version of this article.)

Table 1The summary of correlative data on wettability, solid fraction and solid content of coating composite.

Sample	WCA (°)	Solid fraction (f)	Solid content of composite materials per mL (g)
SP-0	160.43 ± 0.06	0.0297 \pm	0.01613
SP-1	162.17 + 1.12	0.0001 0.0236 +	0.01068
SP-1	162.17 ± 1.12	0.0236 ± 0.0001	0.01008
SP-2	165.14 ± 1.41	0.0174	0.01062
SP-3	136.9 ± 2.7	$0.1377~\pm$	0.01057
		0.0002	

droplet was slowly lifted upward. As a result, a non-wetting behavior was observed; not even a small portion of the droplet remained on the surface of the SP-2 sample.

3.3. Chemical analysis

Fig. 4a depicts the FT-IR spectra for all fabricated samples. The absorption peaks observed at 447 cm⁻¹ and 1058 cm⁻¹ are attributed to the Si-O-Si bond of the silica surface, which were detected before and after the modification of the asymmetric stretching vibrations in the PDMS matrix, respectively. The Si-C bond from the Si-CH₃ group in the PDMS content appears at 841 cm⁻¹, with a higher peak intensity observed in HSS-PDMS coatings compared to the HSS coating [31]. An O-H group from Si-OH or absorbed water is present at 926 cm⁻¹; however, the intensity of these peak decreases in samples SP-1 to SP-3 as they are modified from HSS and HSS-PDMS suspension. This confirms that the hydroxyl groups have been successfully replaced by the trimethylsilyl group of HMDS. Additionally, the stretching bond of C-H from the trimethylsilyl group appears at 2958 cm⁻¹, further confirming that the successful surface modification of silica nanoparticles has been achieved using the trimethylsilyl group of HMDS [32]. Thus, it can be concluded that the silica nanoparticles were modified with HMDS and that the PDMS matrix is adsorbed onto them.

Fig. 4b and 4c-e depict the XPS survey scan and magnified spectra of the Si, O, and C elements in the SP-2 sample. In the magnified Si2p spectra, the prominent peak at 102.5 eV indicates the presence of Si–O–Si bonds, confirming SiO₂ network on the coated surface. The lower peak at 102.37 eV represents Si–C bonding, inferring that the silicon atom is bonded to a methyl group from either

polydimethylsiloxane (PDMS) or hexamethyldisilazane (HMDS) [33]. The close proximity of these two peaks strongly suggests the formation of a composite coating. Additionally, the peak at 532.10 eV indicates the bridging of Si and C atoms by O atoms, which is typical for organosilicon compounds found in PDMS molecules. This peak further confirms that the O atoms are part of both the silicate and organosilicon structures, reinforcing the composite behavior of the coating. The peak at 532.54 eV corresponds to O–Si bonds, providing clear evidence of the presence of the SiO₂ network. In the magnified C1s spectra, the organic compounds C–H/C–C exhibit a high peak around 284.8 eV, which can be attributed to bonding in the methyl group. The lower peak at 285.7 eV represents C–Si bonding, consistent with the trimethylsilyl group from HMDS following the modification of silica nanoparticles, as well as the Si–CH₃ group from PDMS [34].

3.4. Transmittance of the coatings

Fig. 5 presents the transmittance curves for glass, SP-0, SP-1, SP-2, and SP-3 samples. As shown in Fig. 5, all samples demonstrate an average transmittance exceeding 85 % in the wavelength range of 350-1100 nm but lower than bare glass (91.13 %). The SP-0 sample exhibited lower transmittance (85.11 %) among all coatings due to significant shrinkage of the sprayed HSS, which led to the formation of larger particles that acted as barriers to incoming light, resulting in a scattering effect. In contrast, the PDMS-coated samples showed higher transmittance due to better dispersion as well as fixation of silica nanoparticle within PDMS matrix, which did not lead to coating shrinkage during the curing process. Although some particles agglomeration occurred at a small scale, it too acted as a barrier to incoming light. Samples SP-1, SP-2, and SP-3 displayed slight variations in average transparency, registering at 88.31 %, 87.52 %, and 87.09 % respectively within the same wavelength range (350-1100 nm). This indicates that an increase in the amount of PDMS does not significantly affect the transparency of the coatings. Additionally, an optical image of the SP-2 coated glass sample, positioned in front of the colored the colored image to illustrate visibility beyond it, is included as an inset in Fig. 5.

3.5. Durability tests

To evaluate the practical application of outdoor exposure, it is essential to conduct mechanical and chemical tests on the prepared samples. For this purpose, the following tests were carried out: adhesive

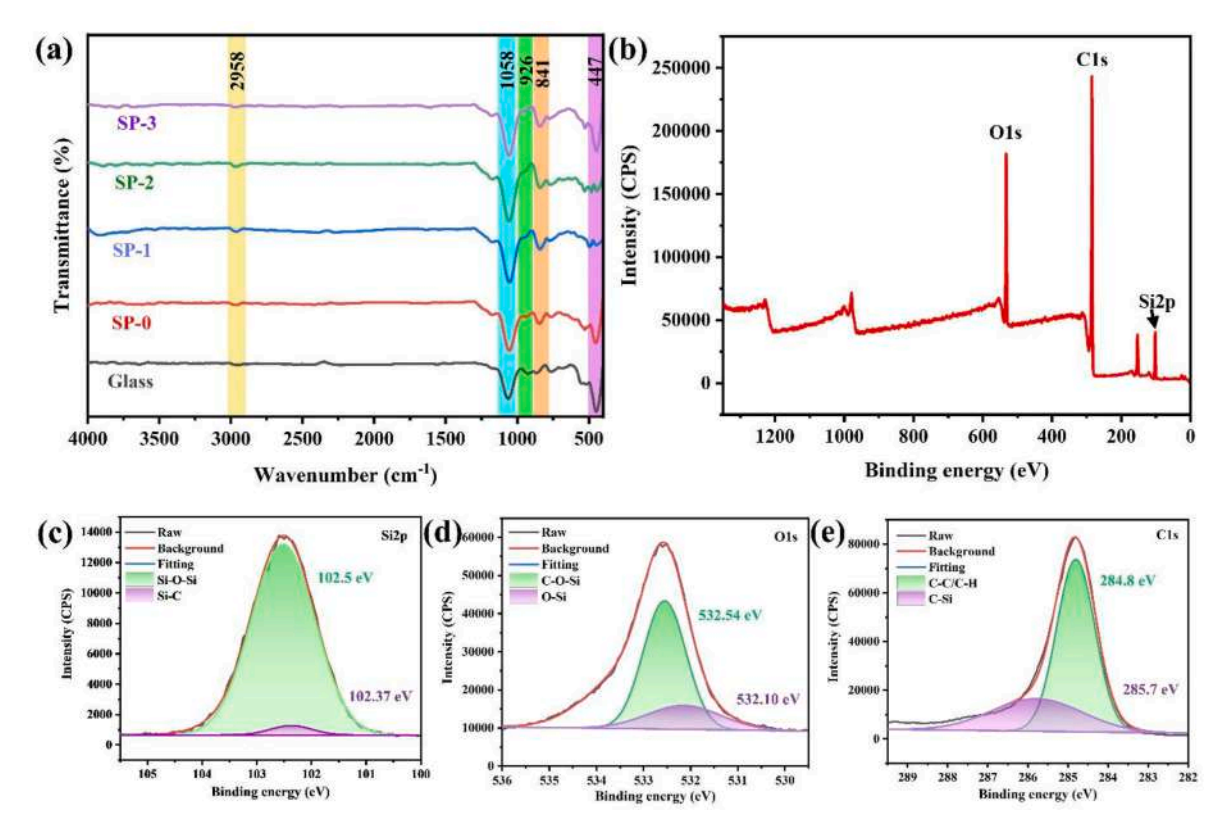


Fig. 4. (a) FT-IR spectra of bare glass, SP-0, SP-1, SP-2 and SP-3, samples. (b) XPS survey spectra of SP-2 sample. High resolution (c) Si2p, (d) O1s and (e) C1s spectra of SP-2 sample.

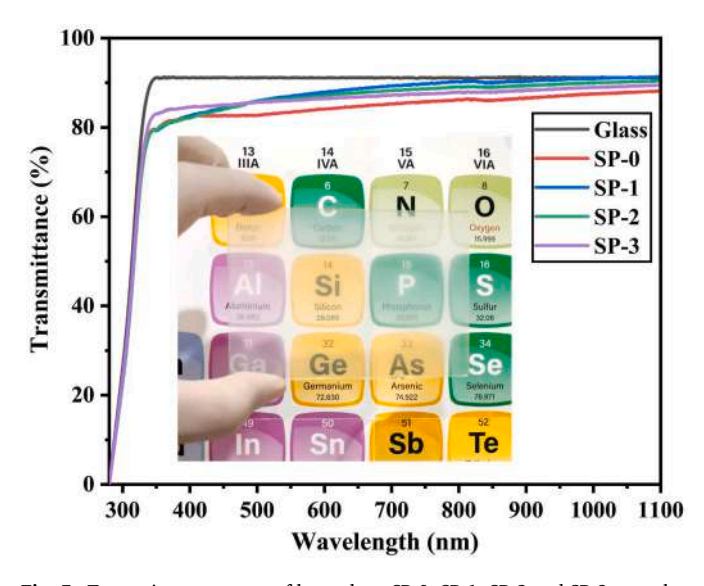


Fig. 5. Transmittance curves of bare glass, SP-0, SP-1, SP-2 and SP-3, samples. An optical image of SP-2 coated glass opposite to periodic table chart.

tape, sandpaper abrasion, pencil hardness, water drop flow, sand flow impact, and the effect of acidic and basic solutions. The adhesive tape test, illustrated in Fig. 6a, was used to assess the adhesion of the prepared coating to the substrate. In this test, adhesive tape was applied to both the HSS and SP-2 samples. A weight of 50 g was rolled over the tape to eliminate any air gaps between the coated surface and the tape. After conducting the test, the samples were examined for wettability. As shown in Fig. 6b, the SP-2 sample maintained its superhydrophobic behavior after four adhesive tape peelings. In contrast, the HSS sample experienced a reduction in its Water Contact Angle (WCA) to 136.68°.

This indicates that the HMDS-modified silica nanoparticles tend to detach readily from the surface. On the other hand, the incorporation of PDMS helped to create a stronger bond with the glass substrate, ensuring good stability even after multiple peelings.

Some external factors can scrape or abrade the coating surface, making it prone to damage. To assess this property, a sandpaper test was conducted. In this test, the coated surface of the sample was placed against the rough side of sandpaper with a grit number of 1500, and a weight of 20 g was added to the substrate (see Fig. 6c). The sample was then dragged for a distance of 15 cm. Fig. 6d illustrates the wettability analysis of the HSS and SP-2 samples. The SP-2 sample lost its superhydrophobic behavior after 30 cm of abrasion, while the HSS maintained its superhydrophobic properties up to 45 cm. During the dragging action, it is possible that nanoparticles were detached from the surface, which may have contributed to the decrease in the water contact angle (WCA).

It is evident that continuous exposure to impacting water droplets may compromise the water-repellent properties of the prepared coating. To assess this, we allowed a steady stream of water droplets to fall on the SP-2 sample (see Fig. 6e). We recorded the WCAs and SAs after an accumulation of 1.6 L of water, with the corresponding trends in wettability shown in Fig. 6f. Even after exposure to 8 L of water, the coated sample retained its superhydrophobic properties, exhibiting a WCA of 151.06 \pm 1.73° and an SA of 25.67 \pm 7.02°. This clearly indicates that the SP-2 sample demonstrated excellent water repellency. A sand particle impact test was conducted to assess the mechanical durability of the coating against collisions with sand particles (see Fig. 7a). In this test, 3 g of sand were allowed to drop from a height of 25 cm. The sand grains reached a velocity of 25 cm/s just before striking the surface. The water contact angles (WCAs) of the coated glass substrate were measured before and after the test, as shown in Fig. 7b. After exposure to the sand impact, damage to the coating occurred, resulting in a reduction of the WCA. This damage suggests that there was partial

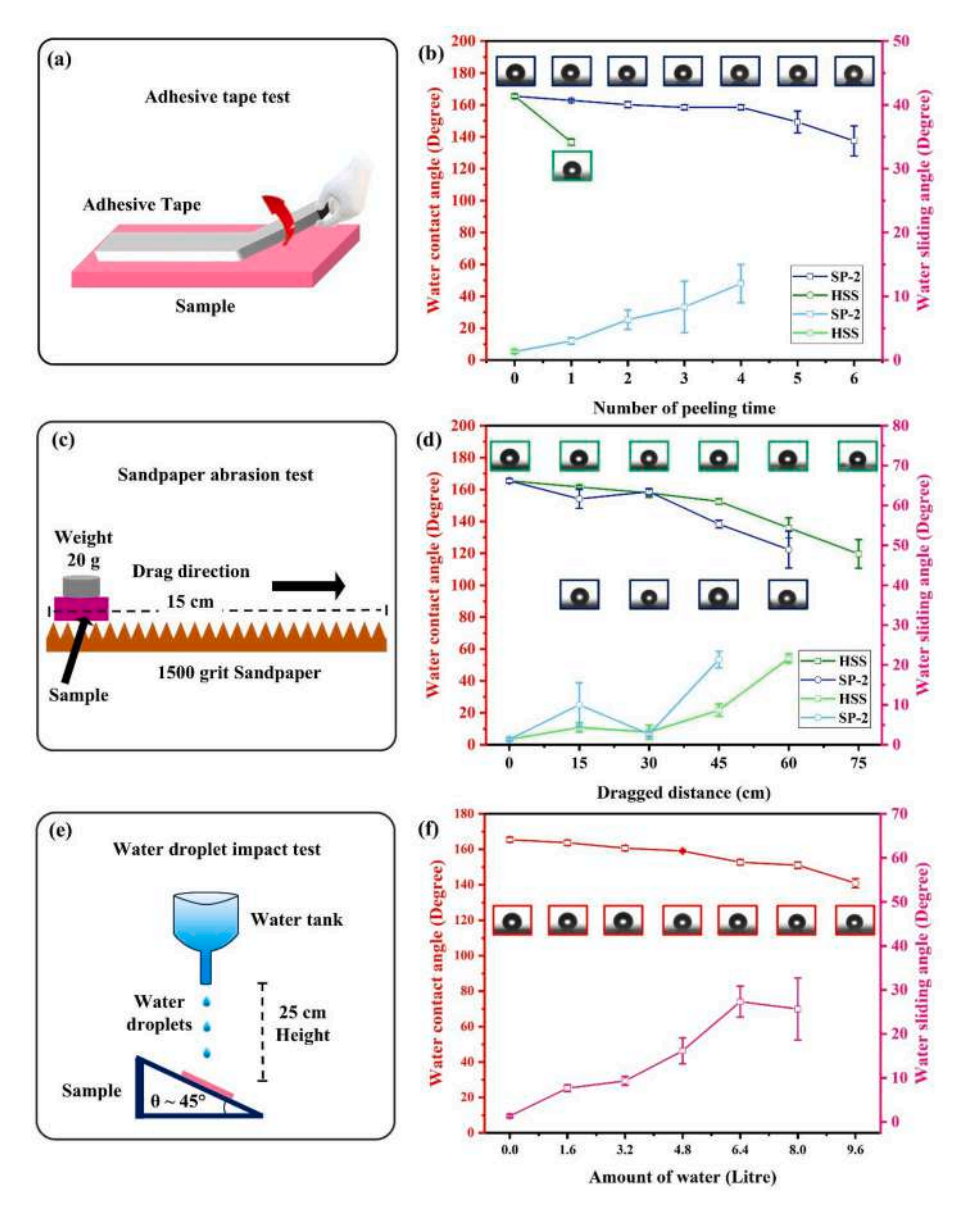


Fig. 6. (a) Schematic and (b) Wettability analysis of SP-2 samples by adhesive tape test. (c) Schematic and (d) Wettability analysis of SP-2 samples by sandpaper abrasion test. (e) Schematic and (f) Wettability analysis of SP-2 samples by water droplet impact test.

destruction of the coated area. Therefore, it can be concluded that the composite materials had a greater affinity for each other than for the glass surface.

In the pencil hardness test, the testing vehicle was driven over the sample using the tip of a 6B pencil on the surface of coating. After conduction of test, it was observed that the dragged area experienced complete removal of the coating, resulting in the absence of any discernible coated layer. Images of the test are shown in Fig. S3(a-c). Figs. 7c and 6d illustrate the schematic diagram and the coated layer before and after the test on the SP-2 sample, respectively. The water repellency of superhydrophobic coating materials is significantly influenced by the rough structure that arises from their specific chemical composition. This composition can be degraded or altered in acidic or basic environments, leading to changes in the original surface morphology of the coating. To assess these changes in morphology and wettability, the prepared samples were immersed in acidic and basic solutions (see Fig. 7e). Solutions with pH levels of 2 and 12 were prepared, and the samples were dipped in these solutions for 30 min intervals while measuring the contact angle (WCA). As illustrated in Fig. 7f, the WCA of the coatings decreased with longer dipping times.

This reduction may result from the dissolution of silica nanoparticles and the degradation of the PDMS polymer under extreme pH conditions. Such changes can also compromise the mechanical integrity of the coating, leading to increased sliding angles for the samples. In this study, the prepared samples lost their superhydrophobicity after 150 min in the pH 2 solution and after 180 min in the pH 12 solution.

3.6. Self-cleaning performance and photovoltaic study

To examine the self-cleaning properties and photovoltaic performance, the SP-2 coated sample was used. The evaluation of the self-cleaning performance involved pouring a solution of charcoal powder mixed with water (see Fig. 8a1-a4) and red dye solution (see Fig. 8b1-b4). A mixture was prepared by combining 2 g charcoal powder with 20 mL of water. This mixture was stirring for 10 min at 500 rpm to achieve a homogeneous solution. The SP-2 sample was tilted at a 10° angle, and the prepared solution was poured onto it. As the solution made contact with the superhydrophobic surface of the SP-2 sample, it rolled off without adhering to any part of the surface. Additionally, when 20 mL of red dye water were poured onto the sample, it similarly rolled off

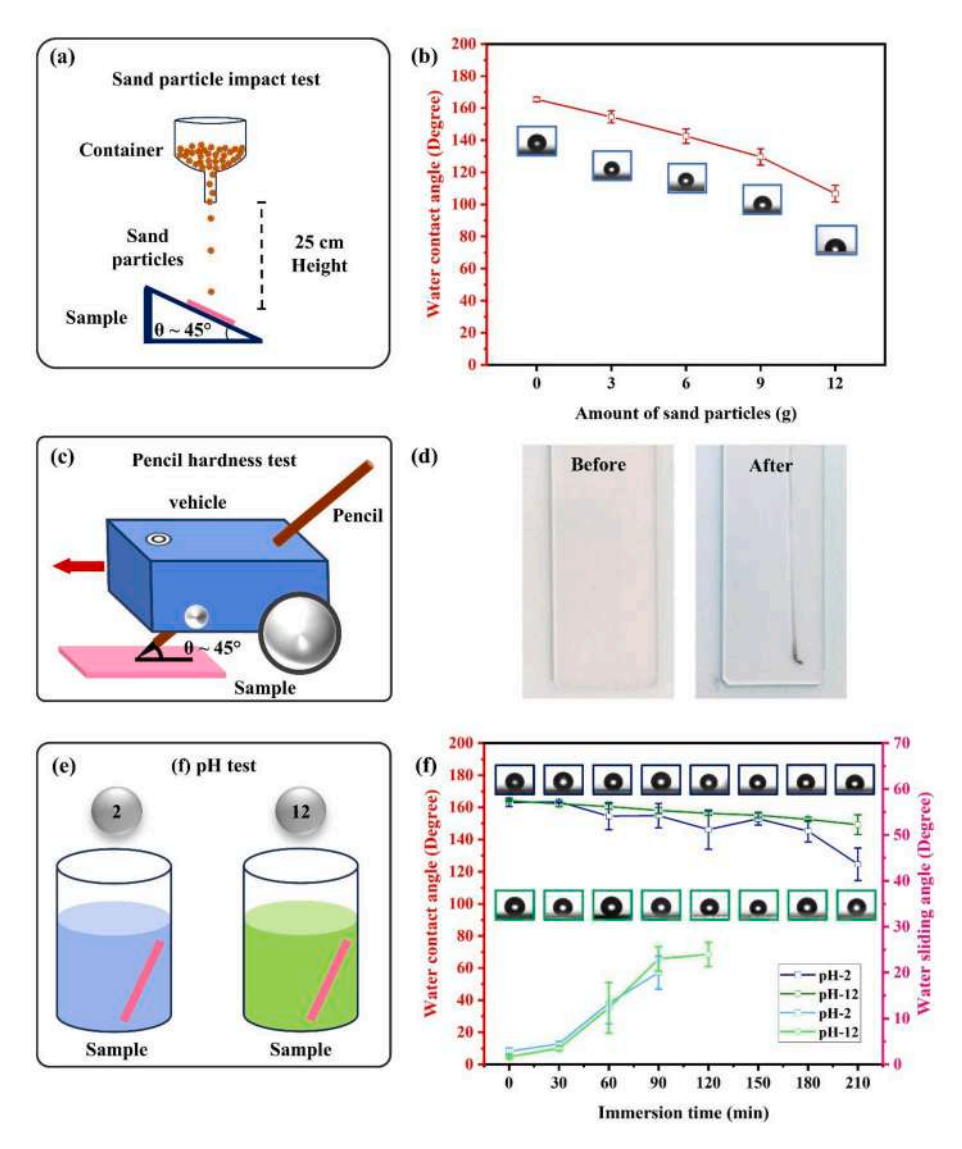


Fig. 7. (a) Schematic and (b) Wettability analysis of SP-2 samples by sand particle impact test. (c) Schematic and (d) optical images of SP-2 samples by pencil hardness test. (e) Schematic and (f) Wettability analysis of SP-2 samples by different pH solutions.

immediately, leaving no traces of red color behind. Consequently, the prepared sample demonstrated outstanding self-cleaning properties.

A small solar cell (99 mm \times 69 mm, purchased from amazon.in, India) was used to evaluate its self-cleaning performance and the effect on efficiency. A cover glass, also measuring 99 mm × 69 mm, was coated with an SP-2 solution and fixed onto the solar cell. The efficiency and fill factor (FF) of the solar cell were calculated by measuring the currents and voltages with both the uncoated and coated cover glasses. Next, fine dust particles (less than 750 µm) were randomly spread on the surface of coated cover glass. Water droplets were introduced onto the coated surface using a 3 mL plastic dropper. When the water droplets reached the coated surface, they began to roll off. During this rolling action, the droplets collected dust particles, leaving the surface clean behind. An increased amount of water led to more thoroughly cleaner surface (see Fig. 9a1-a4). The photovoltaic parameters, including efficiency and FF, were also calculated for each condition during photovoltaic and selfcleaning study. The overall photovoltaic study under different conditions is depicted in Fig. 9b. Initially, uncoated cover glass showed higher efficiency of 6.24 %. When coated glass with transparent superhydrophobic layer applied, the value of efficiency slightly reduced to 4.704 % due to less amount of light scattering as well as reflection. Consequently, during self-cleaning performance, the efficiency of the solar cell regained from 3.192 % to 4.6 % which is nearly equal to the efficiency of the coated cover glass. Although, the coated layer slightly lowers the performance of the solar cell, its self-cleaning ability helps to maintain efficiency in contaminated environment. This is much more valuable for outdoor use. Therefore, the prepared sample can be considered suitable as a cover glass for photovoltaic applications.

4. Conclusion

We have successfully synthesized a composite coating that consists of HMDS-modified silica nanoparticles combined with PDMS using a simple spray deposition technique. A highly stable composite suspension was applied on a glass substrate to achieve the desired properties. The prepared optimized sample exhibited WCA of $165.14 \pm 1.41^{\circ}$ and a SA of $1.33 \pm 0.29^{\circ}$. The optimized sample demonstrated a high transmittance of 87.52 %. Additionally, the coated sample exhibited good mechanical durability through various tests, including adhesive tape, sandpaper abrasion, water droplet impact, exposure to sand particles, pencil hardness, and pH tests. Notably, even after enduring 8 L of water droplet impact, it maintained its superhydrophobic properties. In practical applications, the sample showed excellent self-cleaning capabilities against charcoal powder and colored dyed water, leaving no trace on the

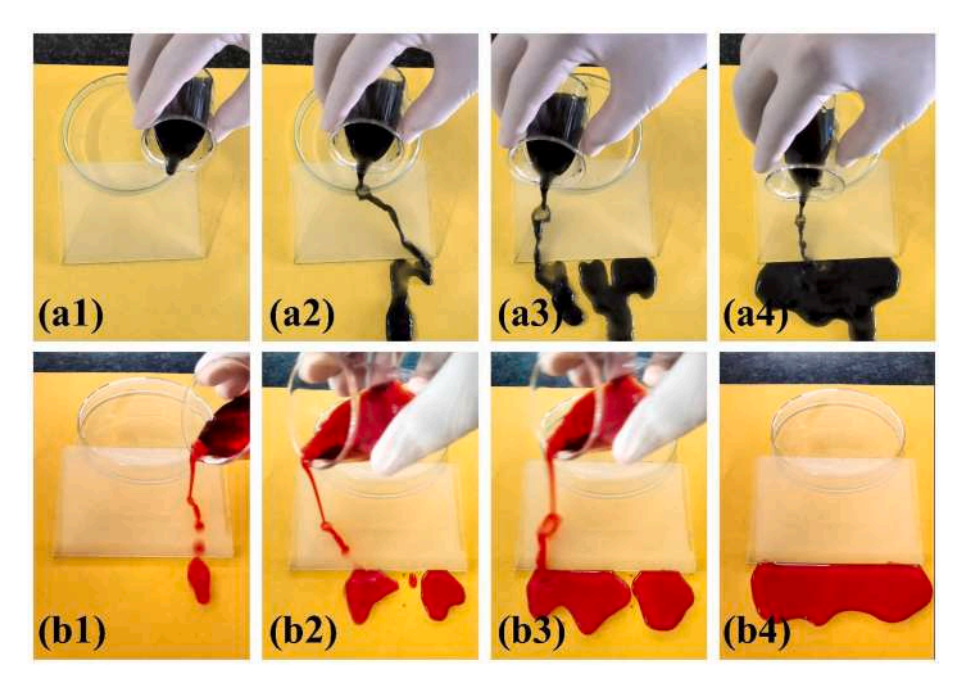


Fig. 8. Self-cleaning performance on SP-2 coated glass by using (a1-a4) charcoal powder-water solution and (b1-b4) red color dyed water. (For interpretation of the references to color in this figure legend, the reader is referred to the Web version of this article.)

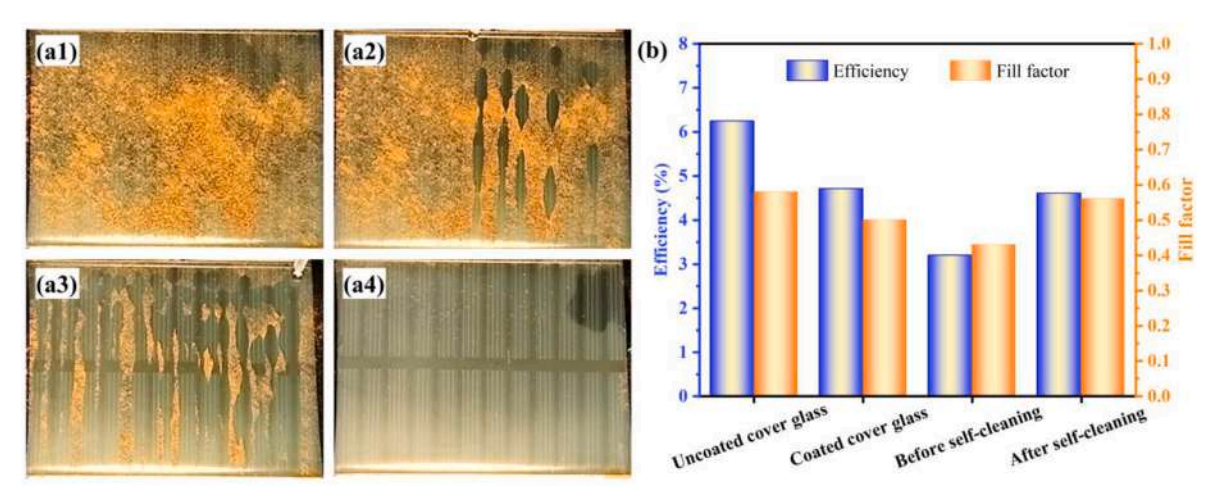


Fig. 9. (a1-a4) Snapshots of self-cleaning process of solar cell. (b) A photovoltaic study of solar cell at different conditions.

surface. Moreover, it retained nearly the same efficiency during photovoltaic tests even after undergoing self-cleaning on the cover glass of a solar cell. Therefore, this type of coating could be valuable in solar energy applications.

CRediT authorship contribution statement

Sagar S. Ingole: Writing – original draft, Methodology, Investigation, Conceptualization. Sudarshan N. Khutale: Methodology. Akshay R. Jundle: Methodology, Investigation. Pradip P. Gaikwad: Methodology, Investigation. Rutuja A. Ekunde: Methodology, Investigation. Rajaram S. Sutar: Writing – original draft, Methodology, Investigation, Conceptualization. Shanhu Liu: Writing – review & editing, Validation. Sanjay S. Latthe: Writing – review & editing, Supervision, Project administration, Funding acquisition, Conceptualization.

Declaration of competing interest

The authors declare that they have no known competing financial interests or personal relationships that could have appeared to influence the work reported in this paper.

Acknowledgments

This work was financially supported by Chhatrapati Shahu Maharaj National Research Fellowship – 2021, Chhatrapati Shahu Maharaj Research Training and Human Development Institute (Sarthi), Pune, Ref. No. CSMNRF-2021/2021-22/896 and Seed Money Scheme from Vivekanand College, Kolhapur (An Empowered Autonomous Institute), Ref. No. VCK/3108/2023-24 dated March 30, 2024.

Appendix A. Supplementary data

Supplementary data to this article can be found online at https://doi.

org/10.1016/j.matchemphys.2025.131757.

Data availability

Data will be made available on request.

References

- B. Zhang, X. Xue, L. Zhao, B. Hou, Transparent superhydrophobic and self-cleaning coating, Polymers 16 (2024) 1876.
- [2] L. Wang, A critical review on robust self-cleaning property of lotus leaf, Soft Matter 19 (2023) 1058–1075.
- [3] Y. Lin, J. Han, M. Cai, W. Liu, X. Luo, H. Zhang, M. Zhong, Durable and robust transparent superhydrophobic glass surfaces fabricated by a femtosecond laser with exceptional water repellency and thermostability, J. Mater. Chem. A 6 (2018) 9049–9056.
- [4] Y. Dou, C. Wu, Y. Fan, Y. Wang, Z. Sun, S. Huang, Y. Yang, X. Tian, Anti-fogging/dry-dust transparent superhydrophobic surfaces based on liquid-like molecule brush modified nanofiber cluster structures, J. Colloid Interface Sci. 664 (2024) 727-735
- [5] Q. He, Y. Xu, F. Zhang, Y. Jia, Z. Du, G. Li, B. Shi, P. Li, M. Ning, A. Li, Preparation methods and research progress of super-hydrophobic anti-icing surface, Adv. Colloid Interface Sci. 323 (2024) 103069.
- [6] R.S. Sutar, S.S. Latthe, A.R. Jundle, P.P. Gaikwad, S.S. Ingole, S. Nagappan, Y. H. Kim, A.K. Bhosale, V.S. Saji, S. Liu, A facile approach for oil-water separation using superhydrophobic polystyrene-silica coated stainless steel mesh bucket, Mar. Pollut. Bull. 198 (2024) 115790.
- [7] R.S. Sutar, S.S. Latthe, X. Wu, K. Nakata, R. Xing, S. Liu, A. Fujishima, Design and mechanism of photothermal soft actuators and their applications, J. Mater. Chem. A 12 (2024) 17896–17922.
- [8] Y. Bai, H. Zhang, Y. Shao, H. Zhang, J. Zhu, Recent progresses of superhydrophobic coatings in different application fields: an overview, Coatings 11 (2021) 116.
- [9] M. Kim, K. Kim, N.Y. Lee, K. Shin, Y.S. Kim, A simple fabrication route to a highly transparent super-hydrophobic surface with a poly(dimethylsiloxane) coated flexible mold, Chem. Commun. (2007) 2237–2239.
- [10] K.L. Cho, I.I. Liaw, A.H.-F. Wu, R.N. Lamb, Influence of roughness on a transparent superhydrophobic coating, J. Phys. Chem. C 114 (2010) 11228–11233.
- [11] N.J. Janowicz, H. Li, F.L. Heale, I.P. Parkin, I. Papakonstantinou, M.K. Tiwari, C. J. Carmalt, Fluorine-free transparent superhydrophobic nanocomposite coatings from mesoporous silica, Langmuir 36 (2020) 13426–13438.
- [12] S. Liu, X. Liu, S.S. Latthe, L. Gao, S. An, S.S. Yoon, B. Liu, R. Xing, Self-cleaning transparent superhydrophobic coatings through simple sol–gel processing of fluoroalkylsilane, Appl. Surf. Sci. 351 (2015) 897–903.
- [13] Y. Wu, L. Dong, Q. Ran, Facile one-step spraying preparation of fluorine-free transparent superhydrophobic composite coatings with tunable adhesion for selfcleaning and anti-icing applications, Appl. Surf. Sci. 649 (2024) 159193.
- Z. Liang, M. Geng, B. Dong, L. Zhao, S. Wang, Transparent and robust SiO2/PDMS composite coatings with self-cleaning, Surf. Eng. 36 (2020) 643–650.
 Y. Liu, X. Tan, X. Li, T. Xiao, L. Jiang, S. Nie, J. Song, X. Chen, Eco-friendly
- [15] Y. Liu, X. Tan, X. Li, T. Xiao, L. Jiang, S. Nie, J. Song, X. Chen, Eco-friendly fabrication of transparent superhydrophobic coating with excellent mechanical robustness, chemical stability, and long-term outdoor durability, Langmuir 38 (2022) 12881–12893.
- [16] H. Zhang, Y.-Q. Liu, S. Zhao, L. Huang, Z. Wang, Z. Gao, Z. Zhu, D. Hu, H. Liu, Transparent and robust superhydrophobic structure on silica glass processed with microstereolithography printing, ACS Appl. Mater. Interfaces 15 (2023) 38132–38142.

- [17] A. Syafiq, B. Vengadaesvaran, N.A. Rahim, A. Pandey, A. Bushroa, K. Ramesh, S. Ramesh, Transparent self-cleaning coating of modified polydimethylsiloxane (PDMS) for real outdoor application, Prog. Org. Coating 131 (2019) 232–239.
- [18] A.G. Leao, B.G. Soares, A.A. Silva, E.C. Pereira, L.F. Souto, A.C. Ribeiro, Transparent and superhydrophobic room temperature vulcanized (RTV) polysiloxane coatings loaded with different hydrophobic silica nanoparticles with self-cleaning characteristics, Surf. Coating. Technol. 462 (2023) 129479.
- [19] C. Li, G. Chang, S. Wu, T. Yang, B. Zhou, J. Tang, L. Liu, R. Guan, G. Zhang, J. Wang, Y. Yang, Highly transparent, superhydrophobic, and durable silica/resin self-cleaning coatings for photovoltaic panels, Colloids Surf. A Physicochem. Eng. Asp. 693 (2024) 133983.
- [20] H. Salehi, A. Eshaghi, M. Rezazadeh, H. Zabolian, Antireflective and anti-dust modified silica based thin film on solar cell cover glass, J. Alloys Compd. 892 (2022) 162228.
- [21] F. Saeedi, A. Eshaghi, M. Ramazani, H. zabolian, A.N. Esfahani, Transparent hydrophobic and anti-icing thin films based on polydimethylsiloxane-SiO₂ nanoparticles co-modified with TMMS and HDMS, J. Alloys Compd. 1022 (2025) 170021
- [22] H. Henschel, A.M. Schneider, M.H. Prosenc, Initial steps of the sol-Gel process: modeling silicate condensation in basic medium, Chem. Mater. 22 (2010) 5105–5111
- [23] T. Domenech, S.S. Velankar, On the rheology of pendular gels and morphological developments in paste-like ternary systems based on capillary attraction, Soft Matter 11 (2015) 1500–1516.
- [24] S. Turkoglu, J. Zhang, H. Dodiuk, S. Kenig, J.A. Ratto Ross, S.A. Karande, Y. Wang, N. Diaz Armas, M. Auerbach, J. Mead, Structure-property relationships for fluorinated and fluorine-free superhydrophobic crack-free coatings, Polymers 16 (2024).
- [25] X. Gong, S. He, Highly durable superhydrophobic polydimethylsiloxane/silica nanocomposite surfaces with good self-cleaning ability, ACS Omega 5 (2020) 4100–4108.
- [26] I. Protsak, E. Pakhlov, V. Tertykh, Z.-C. Le, W. Dong, A new route for preparation of hydrophobic silica nanoparticles using a mixture of poly(dimethylsiloxane) and diethyl carbonate, Polymers 10 (2018) 116.
- [27] K. Jeevajothi, D. Crossiya, R. Subasri, Non-fluorinated, room temperature curable hydrophobic coatings by sol–gel process, Ceram. Int. 38 (2012) 2971–2976.
- [28] M. Luo, X. Sun, Y. Zheng, X. Cui, W. Ma, S. Han, L. Zhou, X. Wei, Non-fluorinated superhydrophobic film with high transparency for photovoltaic glass covers, Appl. Surf. Sci. 609 (2023) 155299.
- [29] H. Salehi, A. Eshaghi, M. Rezazadeh, Aging time effect on wettability and transparency of Hexamethyldisilazane-modified silica thin film, Opt. Mater. 148 (2024) 114911.
- [30] S.-D. Wang, Y.-Y. Shu, Superhydrophobic antireflective coating with high transmittance, J. Coating Technol. Res. 10 (2013) 527–535.
- [31] R.S. Sutar, B. Shi, S.S. Kanchankoti, S.S. Ingole, W.S. Jamadar, A.J. Sayyad, P. B. Khot, K.K. Sadasivuni, S.S. Latthe, S. Liu, Development of self-cleaning superhydrophobic cotton fabric through silica/PDMS composite coating, Surf. Topoer, Metrol. Prop. 11 (2023) 045004.
- [32] B. Thasma Subramanian, J.P. Alla, J.S. Essomba, N.F. Nishter, Non-fluorinated superhydrophobic spray coatings for oil-water separation applications: an ecofriendly approach, J. Clean. Prod. 256 (2020) 120693.
- [33] X. Su, H. Li, X. Lai, L. Zhang, J. Wang, X. Liao, X. Zeng, Vapor-liquid sol-gel approach to fabricating highly durable and robust superhydrophobic polydimethylsiloxane@ silica surface on polyester textile for oil-water separation, ACS Appl. Mater. Interfaces 9 (2017) 28089–28099.
- [34] Y. Wu, Y. Shen, J. Tao, Z. He, Y. Xie, H. Chen, M. Jin, W. Hou, Facile spraying fabrication of highly flexible and mechanically robust superhydrophobic F-SiO₂@ PDMS coatings for self-cleaning and drag-reduction applications, New J. Chem. 42 (2018) 18208–18216.